Process Safety and Environmental Protection 162 (2022) 1015–1024

Contents lists available at ScienceDirect

Process Safety and Environmental Protection

journal homepage: www.elsevier.com/locate/psep

Application of a hybrid mechanistic/machine learning model for prediction of nitrous oxide (N_2O) production in a nitrifying sequencing batch reactor

Mohamad-Javad Mehrani[a,*], Faramarz Bagherzadeh[b], Min Zheng[c], Przemyslaw Kowal[a], Dominika Sobotka[a], Jacek Mąkinia[a]

[a] Faculty of Civil and Environmental Engineering, Gdansk University of Technology, ul. Narutowicza 11/12, 80-233 Gdansk, Poland
[b] Faculty of Mechanical Engineering, Gdansk University of Technology, ul. Narutowicza 11/12, 80-233 Gdansk, Poland
[c] Australian Centre for Water and Environmental Biotechnology, The University of Queensland, St Lucia, QLD 4072, Australia

ARTICLE INFO

Article history:
Received 6 September 2021
Received in revised form 25 February 2022
Accepted 24 April 2022
Available online 30 April 2022

Keywords:
Prediction accuracy
Mechanistic model
Machine learning
Nitrous oxide
Nitrification
GHG mitigation

ABSTRACT

Nitrous oxide (N_2O) is a key parameter for evaluating the greenhouse gas emissions from wastewater treatment plants. In this study, a new method for predicting liquid N_2O production during nitrification was developed based on a mechanistic model and machine learning (ML) algorithm. The mechanistic model was first used for simulation of two 15-day experimental trials in a nitrifying sequencing batch reactor. Then, model predictions (NH_4-N, NO_2-N, NO_3-N, MLSS, MLVSS) along with the recorded online measurements (DO, pH, temperature) were used as input data for the ML models. The data from the experiments at 20 °C and 12 °C, respectively, were used for training and testing of three ML algorithms, including artificial neural network (ANN), gradient boosting machine (GBM), and support vector machine (SVM). The best predictive model was the ANN algorithm and that model was further subjected to the 95% confidence interval analysis for calculation of the true data probability and estimating an error range of the data population. Moreover, Feature Selection (FS) techniques, such as Pearson correlation and Random Forest, were used to identify the most relevant parameters influencing liquid N_2O predictions. The results of FS analysis showed that NH_4-N, followed by NO_2-N had the highest correlation with the liquid N_2O production. With the proposed approach, a prompt method was obtained for enhancing prediction of the liquid N_2O concentrations for short-term studies with the limited availability of measured data.

1. Introduction

Nitrous oxide (N_2O) is one of the most significant greenhouse gases (GHGs) with an extremely high global warming potential (GWP), which is almost 300 times higher than that of carbon dioxide (IPCC, 2014). Wastewater treatment plants (WWTPs) are responsible for 3–5% of worldwide anthropogenic N_2O emissions (Mannina et al., 2019). In WWTPs, N_2O is primarily produced during biological nitrogen removal processes, including autotrophic nitritation (aerobic ammonium oxidation to nitrite) and heterotrophic denitritation (reduction of nitrite) (Su et al., 2019).

Moreover, carbon footprint (CF) is a measure of GHG emissions (Delre et al., 2019). The amount of N_2O produced in wastewater treatment operations has a significant impact on the overall CF of WWTPs (Maktabifard et al., 2020). High shares of N_2O emissions in the CF have been observed in biological nutrient removal (BNR) plants (Koutsou et al., 2018). Hence, an accurate estimation of N_2O can help in better understanding of the process behavior and consequently, mitigation and control of this GHG in WWTPs. An N_2O emission factor is a vital indicator of the long-term sustainability of WWTPs and environmental protection (Chen et al., 2020a; Vasilaki et al., 2019).

Mathematical models are a strong tool for process simulation, prediction, and optimization (Wisniewski et al., 2018). There are two possible approaches for N_2O modeling, including mechanistic models and machine learning (ML) techniques. In the area of wastewater treatment, the Activated Sludge Models (ASMs) (Henze et al., 2006) are the most common mechanistic models, which mathematically describe a hypothetical base for biological wastewater treatment processes. There has been a growing number of successful applications of mechanistic modeling for N_2O prediction

* Corresponding author.
E-mail address: mohammad-javad.mehrani@pg.edu.pl (M.-J. Mehrani).

https://doi.org/10.1016/j.psep.2022.04.058
0957-5820/

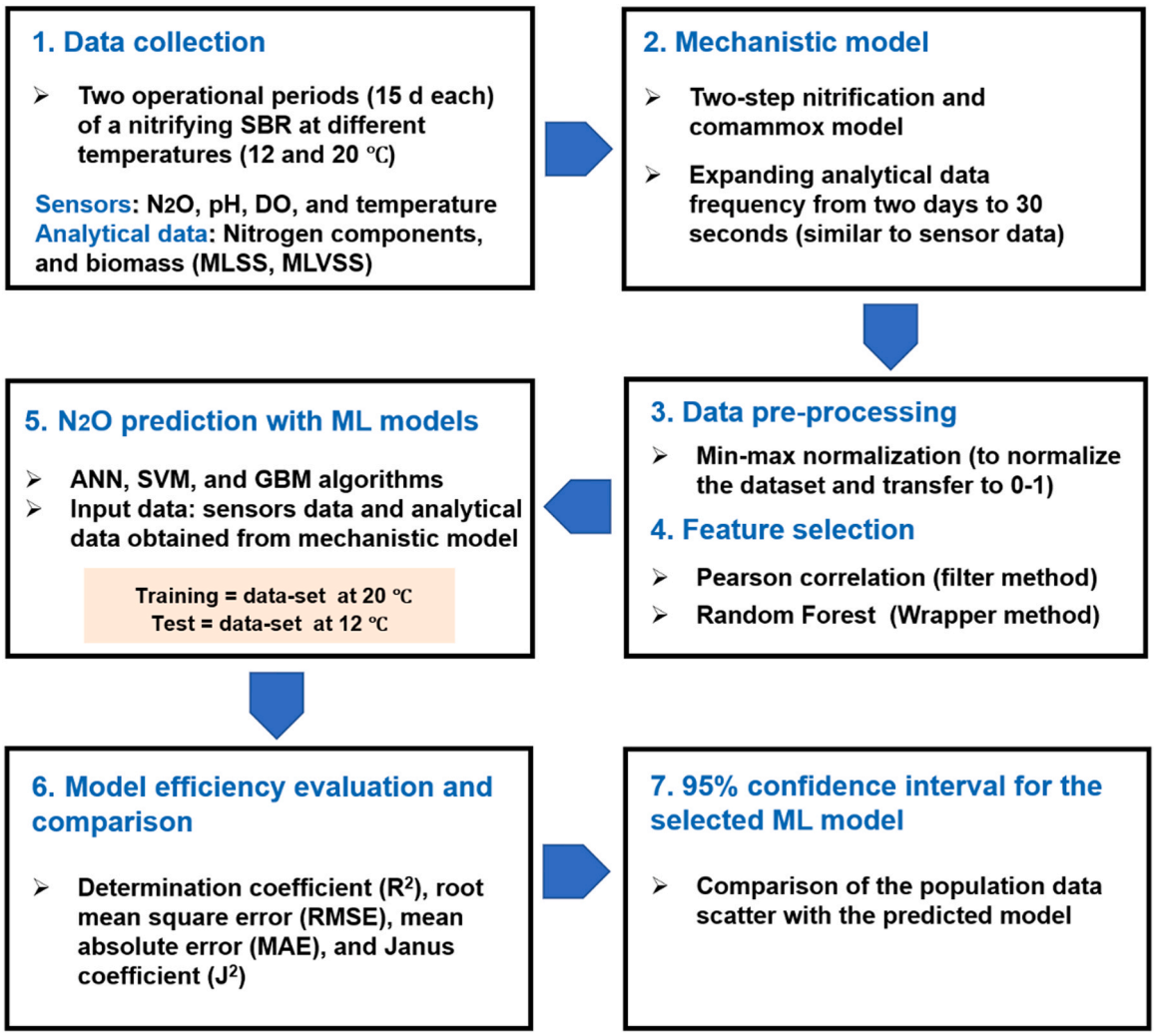

Fig. 1. The procedure of the implementation, training and test, and comparison of prediction ML models.

in real WWTPs (Massara et al., 2018; Su et al., 2019; Wang et al., 2016; Zaborowska et al., 2019). However, these models have a few limitations. First of all, prediction of N_2O requires an extensive knowledge of biological nitrogen transformations for model identification and calibration (Zaborowska et al., 2019). No generic mechanistic model is available, while various expansions and modifications have been added to the existing models (Vasilaki et al., 2019; Chen et al., 2020b). In addition, the traditional mechanistic models are over parameterized, highly sensitive to the changes in operational condition, and demand extensive efforts for calibration and validation. A calibration procedure for N_2O is especially challenging as N_2O is only an intermediate in the nitrogen transformation chain and its contribution to the nitrification process is low (Hwangbo et al., 2021).

On the other hand, ML is a tool for data analysis that can learn from input data and make decisions accordingly without any process equations and pathways (Al-Jamimi et al., 2018). ML algorithms recognize a specific pattern (during a training process) based on defined data (input data) for the prediction and/or classification purposes, which results in a more accurate output (Bagherzadeh et al., 2021; Osarogiagbon et al., 2021). In WWTPs, the ML prediction models have primarily been used for modeling influent/effluent wastewater characteristics. Those models are mainly artificial neural network (ANN) (Ryan et al., 2004; Shaahmadi et al., 2017) and support vector machine (SVM) (Alejo et al., 2018; Shaahmadi et al., 2017; Vasilaki et al., 2020b), while gradient boosting machine (GBM) has been used less frequently (Bagherzadeh et al., 2021). In addition, there are very limited studies on hybrid models (mechanistic models combined with the ML techniques) for forecasting influent/effluent wastewater components (Haimi et al., 2013; Hvala and Kocijan, 2020), but there has been no such a hybrid model applied for N_2O prediction yet.

In terms of N_2O, a predictive ML model of N_2O emission, based on experimental data from an anoxic/aerobic bioreactor with ANN, was proposed by Sun et al. (2017). Moreover, two algorithms, including random forest (RF) and SVM, were used by Vasilaki et al. (2020b) to determine N_2O emission factors. The SVM models performed better than RF in the training of the model to predict the expected range of N_2O emission in WWTPs. Very recently, data-driven-based models, including long short-term memory (LSTM) and deep neural network, have been used to predict liquid N_2O concentrations by big data from a full-scale WWTP (Hwangbo et al., 2021).

In this study, a predictive hybrid model for liquid N_2O production was developed based on the data from a laboratory-scale nitrifying sequencing batch reactor (SBR). The new model overcame limitations of the pure mechanistic models or ML algorithms. This approach includes two major steps: **i)** mechanistic model simulation for expanding the short-term experimental data into an extensive data set with a very small interval (similar to the recordings of a liquid N_2O sensor, and **ii)** liquid N_2O predictions using three powerful ML algorithms (ANN, SVM, and GBM) to achieve a highly accurate model by producing input data from the previous step. To the

Table 1
Statistical summary report of the input and output data used for the ML algorithms.

Data	Function	Mechanistic model predictions					Online measurements			
		NH_4-N (mg N/L)	NO_3-N (mg N/L)	NO_2-N (mg N/L)	MLSS (mg/L)	MLVSS (mg/L)	DO (mg O_2/L)	Temp (℃)	pH -	N_2O (mg N/L)
Training data	Min	2.00	4.86	4.92	545.4	350.9	0.20	18.74	7.11	0.00
	Max	49.06	37.29	12.97	2151.0	1351.0	2.22	21.51	8.35	0.57
	Mean	31.81	29.45	8.44	1176.5	744.54	0.61	20.08	7.55	0.15
Testing data	Min	0.00	19.22	0.00	545.4	350.9	0.150	11.74	7.09	0.00
	Max	119.30	127.40	53.33	2151	1351.0	2.17	13.11	8.65	0.11
	Mean	38.89	93.11	22.57	1176	744.54	0.65	12.29	7.45	0.07

best of our knowledge, this hybrid approach has been used for the first time for N_2O prediction in short-term studies. This research demonstrates a prompt method for enhancing prediction of liquid N_2O concentrations with the limited availability of measured data.

2. Materials and methods

The modeling procedure includes two separate steps for the mechanistic model and ML algorithms. The first step was carried out for expanding the data-set, i.e., converting the communication interval of analytical data similar to the sensor data. The complete process of calibration and validation of the mechanistic model using GPS-X 8.0 software can be found in our previous study (Mehrani et al., 2021). In the second step, liquid N_2O concentrations were predicted by three ML algorithms based on the data generated by the mechanistic model. The diagram in Fig. 1 presents the full modeling/prediction approach.

2.1. Data collection for simulation

Two series of long-term washout experimental trials were carried out in the SBR. The experiments aimed at washing out NOB at decreasing solids retention times (SRTs) from 4d to 3d. The inoculum biomass was taken from the "Czajka" WWTP in Warsaw, Poland during winter and summer periods. The working volume of the SBR was 10 L and the reactor was operated for 15 days at the temperatures typical for winter and summer conditions, i.e., 12 °C and 20 °C. The temperature was kept constant during the experiment with a tolerance of ± 1.5 for 20 ℃ and ± 1.0 for 12 ℃.

The experiments at 20 °C and 12 °C were selected for training and testing the ML algorithms, respectively (Table 1). The initial mixed liquid suspended solids (MLSS) and volatile fraction (MLVSS) concentrations were approximately 2000 mg/L and 1200 mg/L for the experiment at 12 °C, and 2500 mg/L and 1500 mg/L for the experiment at 20 °C.

The SBR was fed with ammonium-rich synthetic wastewater, including tracer elements, but without organic substrate (Mehrani et al., 2021). The volumetric nitrogen loading rates (NLRs) were kept stable at 0.02 ± 0.01 and 0.05 ± 0.01 g N/(L·d) at 12 °C and 20 °C, respectively. During the experiments, pH, temperature, DO concentration, and liquid N_2O concentration were recorded every 30 s by online sensors (Table 1).

2.2. Simulations with a mechanistic model

For both experiments, simulations with the mechanistic model (two-step nitrification with comammox) were run with a communication time of 30 s (similar to the online sensor data). GPS-X 8.0 software (Hydromantis, 2021) was used as a simulation platform. The details of calibration and validation of the mechanistic model can be found in the previous study (Mehrani et al., 2021).

Simulation results, including nitrogen species (NH_4-N, NO_2-N, and NO_3-N) and biomass components (MLSS, MLVSS), were selected as input data (> 50k data for each parameter) of the ML algorithms. Table 1 shows a brief representation of the acquiesced input data set from the mechanistic model and online sensors data, separately for the training and testing data sets.

2.3. Data pre-processing for ML algorithms

Before ML prediction, the data obtained from the mechanistic model and online sensors were subjected to data engineering, i.e., cleaning the information with care taken to the missing or irregular records (Halim et al., 2021; Ranjan et al., 2021). Moreover, input data for training and testing the models were normalized and scaled between 0.0 and 1.0 values as:

$$\mathrm{Xn} = \frac{Xi - Xmin}{Xmax - Xmin} \tag{1}$$

where Xn is normalized data, Xmax, and Xmin are the maximum and minimum values of the considered variable, and Xi is the value of the variable in each record. The normalization helps assign relevant weights for the ML models considering the value of each feature.

2.4. Feature selection for ML algorithms

Pearson correlation. Pearson correlation coefficient (PCC) is a feature selection (FS) filter method and is considered one of the most straightforward FS strategies. The PCC defines the linear relationship between two variables that range from + 1 to − 1, with 1 indicating total positive correlation, 0 indicating no correlation, while − 1 showing the negative correlation (Ali et al., 2021; Alver and Altaş, 2017). The PCC is computed as:

$$\sigma_{ij} = \frac{Cov(f_i, f_j)}{\sqrt{Var(f_i)Var(f_j)}} \tag{2}$$

where σ_{ij} is a correlation coefficient between a given feature f_i and all other features of the data set f_j, *Cov* is covariance, and *Var* is a variance.

Random Forest. The random forest (RF) is a ML filter method for ranking input variables according to their significance (Breiman, 2001). In this technique, several decision trees are created using random feature extraction and data set observations. The trees are de-correlated as a result of this random collection of records and features (bootstrapping). Each bootstrap is used to train a tree when there is a T number of trees in total (Breiman, 2001; Masmoudi et al., 2020). A small portion of data in each bootstrap is kept out of the box (oob_i) to evaluate the feature importance. Moreover, feeding the input feature f observations randomly to the tree will result in oob_i^f. Ultimately, the tree is able to predict the new values of the box by applying the mean squared error, $MSE(oob_i^f)$, and the feature importance is calculated as:

$$I(f) = \frac{1}{T}\sum_{i=1}^{T}\frac{MSE(oob_i^f) - MSE(oob_i)}{MSE(oob_i)} \tag{3}$$

Higher importance values show that the feature is more relevant to the target, and it can improve the prediction output.

2.5. Prediction of liquid N_2O concentrations with ML models

After mechanistic modeling and data pre-processing, the ML algorithms were constructed for liquid N_2O prediction during the two experimental trials in the SBR. Python 3.8 open source programming language was used, while applying various libraries, such as Pandas, Matplotlib, Keras, and Scikitlearn. Each prediction algorithm is outlined in the following subsections and the details are given in the SI.

ANN algorithm. To locate the useful connection among dependent and independent variables, fully connected neural networks can be built up for prediction analysis (Yegnanarayana, 2009). For each neuron, a linear equation between its input and output is assumed. Due to the unpredictability of a non-linear model, more neurons are expected to anticipate the objective variable with a satisfactory precision (Eq. (4)):

$$y = \sigma(\beta_0 + \beta_1 X_1 + \beta_2 X_2 + ...+\beta_n X_n) \tag{4}$$

where y is the output of the ANN, σ is the sigmoid function, X_i is the input number in each neuron, β_0 is the sum of biases of each neuron, and β_i is the weight (trainable parameter) of the neuron.

An ANN is a multilayer perceptron (MLP) with three layers: input, hidden, and output (Kazemi et al., 2021). In a straightforward approach, the number of input layer neurons is the same as the size of a model dimensionality. To guarantee a smooth and precise link between the layers, the rectified linear unit (ReLU) technique was utilized for selecting a suitable number of the layers. The constructed ANN algorithm consists of seven input layers (MLSS was ignored due to a high correlation with MLVSS), three hidden layers with 10, 10, and 5 neurons respectively, and one neuron in the output layer. The optimization algorithm and the loss criterion were Adam and MSE, respectively.

SVM algorithm. The SVM is a versatile ML model that can do linear and nonlinear predictions, and even outlier detection (Vapnik et al., 1995; Géron, 2019). This method was originally designed to solve classification problems before being expanded to solve prediction problems. Since the cost function criteria for model building do not refer to attribute values that lie outside the margin, a model generated by the SVM is extremely depended on the subset of training data (Arshad et al., 2021). As shown in Fig S1, data points outside of the decision boundary will be ignored for developing the hyperplane (removing outliers). Similarly, the SVM model is only based on a subset of the training results (Vapnik et al., 1995). Any training data which are close to the model prediction (hyperplane) are ignored by the cost function method to prevent overfitting issues (Steinwart and Christmann, 2008).

SVM prediction (SVR) is a supervised learning model that uses the same SVM (classification) manner with minor editions. As it is difficult to predict a real number (infinite possibilities), a margin of error is considered for the prediction. The SVR transforms an input matrix to a higher dimensional feature space via a kernel. The following equation expresses the non-linear SVR function $F(x)$ in a mathematical format (Eq. 5) (Awad and Khanna, 2015; Park et al., 2021):

$$F(x) = \sum_{i=1}^{M} (\alpha_i - \alpha_i^*) \quad K(X_i, X) + \delta \tag{5}$$

where M is the number of training records, α_i , α_i^* are Lagrange multipliers, K is the transformation kernel that contains the dot product of mapped vectors of the support vectors (X_1 .... X_i), and δ is the sum of biases (Smola and Schölkopf, 2004).

GBM algorithm. The gradient boosting machine (GBM) is a kind of decision-tree ML model with a distinct ensemble formation of supportive technique (Ayyadevara, 2018). In this method, new trees are added to the ensemble sequentially based on the overall ensemble prediction error (Natekin and Knoll, 2013). The estimation error for the dependent variable shrinks continuously by adding new trees until it reaches the highest possible accuracy (Bagherzadeh et al., 2021). The algorithm produces a new decision tree to minimize the prediction error, and finally, the output of all trees will be aggregated:

$$Data \quad set = \{x^i, Y^i\} \quad {}^{N}_{i=1} \quad Minimizing \quad \left\| \sum_{i=1}^{N} L(F(x^i), Y^i) \right\| \tag{6}$$

where N is the number of records, x^i are independent variables, Y^i is the target variable in the training data set, L is the error function, and $F(x^i)$ is the model output (Xenochristou et al., 2020).

The ultimate goal of GBM is to develop one strong model from several weak and smaller learning models (decision tree models). Considering Eq. (6), the GBM algorithm takes the training data and tries to minimize the error value. Decision trees divide the data set at each branch (node) to maximize the entropy. Each tree has several nodes and will split the data set until fulfilling the given hyperparameters (maximum tree depth).

Adjusting the hyper-parameters is a crucial step in designing a GBM model. Therefore, after many trial-and-error attempts, the following values were used in this study: a learning rate of 0.05, the number of 2000 trees for the forest, subsampling of 0.8, a tree depth of 6, a min sample leaf of 50, and minimum split samples as a 600.

2.6. Evaluation and comparison of the efficiency of ML models

The model performance can be evaluated with statistical methods. The dependent variable data are assumed as $y_1, y_2...y_n$ with the mean value $\bar{y}$ and estimated values of this variable as $f_1, f_2...f_n$ (collectively known as y_i and f_i). Then the sum square of residuals (SS_{res}) and the total sum of squares (SS_{tot}) are calculated, and the coefficient of determination (R-squared) indicates "goodness-of-fit" between the predicted feature and real values. Moreover, the mean absolute error (MAE), root mean square error (RMSE), and Janus coefficient describe the model errors and accuracy (Eqs. (7)–(12)) (Hauduc et al., 2015; Verma et al., 2013):

$$SS_{tot} = \sum_i (y_i - \bar{y})^2 \tag{7}$$

$$SS_{res} = \sum_i (y_i - f_i)^2 \tag{8}$$

$$R^2 = 1 - \frac{SS_{res}}{SS_{tot}} \tag{9}$$

$$MAE = \frac{1}{n} \sum_i (y_i - f_i) \tag{10}$$

$$RMSE = \sqrt{\frac{SS_{res}}{n}} \tag{11}$$

$$J^2 = \sqrt{\frac{RMSE^2_{validation}}{RMSE^2_{calibration}}} \tag{12}$$

where y_i is the observed data in the data set, f_i is the model prediction, $\bar{y}$ is the mean value of the observed data, and n is the number of observation samples.

2.7. Calculation of the confidence interval for the selected ML model

The confidence interval (CI) is a valuable measure to indicate the estimated range of error. In this study, there is a large number of observations with a normal error distribution. Therefore, the 95% CI was calculated with a z-score (Eq. (13)), considering that the standard deviation of the population is known due to having a high number of records (Hogg, 2012):

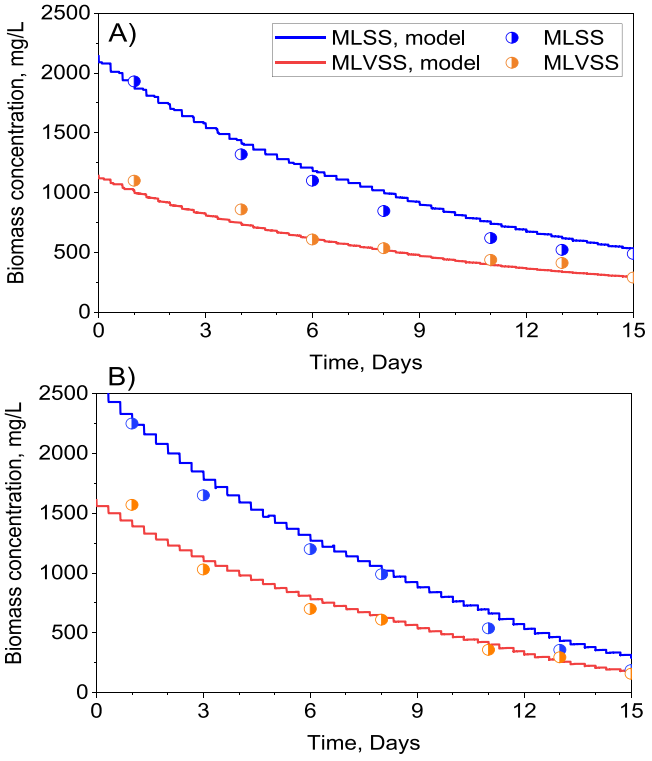

Fig. 2. Measured vs. predicted MLSS and MLVSS concentrations by the mechanistic model: A) Experiment at 12 °C, B) Experiment at 20 °C.

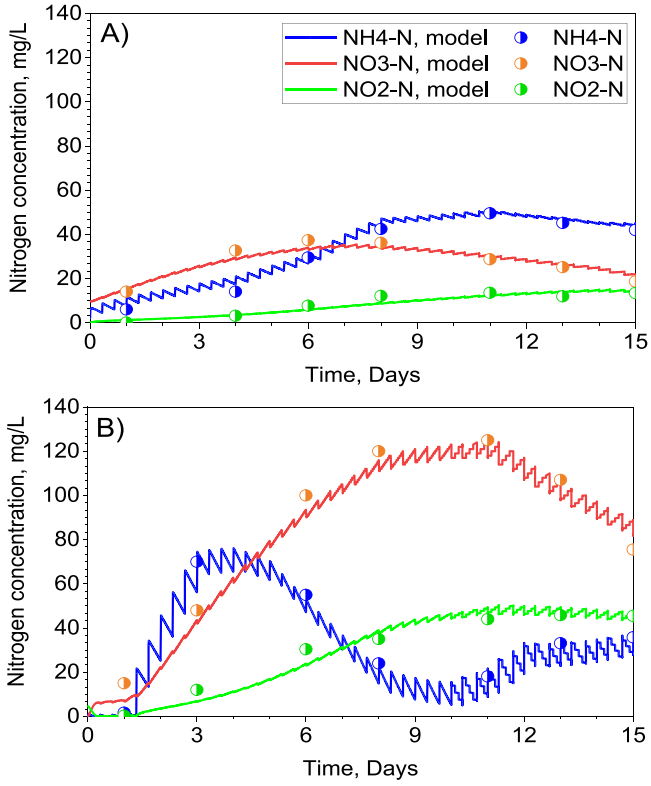

Fig. 3. Measured vs. predicted concentrations of nitrogen species by the mechanistic model: A) Experiment at 12 °C, B) Experiment at 20 °C.

$$CI = \bar{X} \pm z\frac{\sigma}{\sqrt{n}} \quad (13)$$

where $\bar{X}$ is the sample mean, z is the value from the standard normal distribution for the selected confidence level, σ is the standard deviation, and n is the total number of observations. If all the test points are within the 95% CI, it indicates a high level of precision (Abbas et al., 2018).

3. Results

3.1. Predictions of the mechanistic model (ML input data acquisition)

The results of predicted biomass concentrations (MLSS and MLVSS) and nitrogen species by the calibrated mechanistic model are shown in Fig. 2 and Fig. 3, respectively. The MLSS and MLVSS concentrations revealed a decreasing trend in both experiments due to the continuous biomass washout conditions (Fig. 2). Concerning the nitrogen species, in the experiment at 12 °C (Fig. 3a), NO_3-N started to dilute after the first week resulting from biomass and NOB washout, while NO_2-N stabilized at around 12–15 mg N/L to the end of the experiment. In the experiment at 20 °C (Fig. 3b), the NLRs were approximately doubled (0.05 ± 0.01 g N/(L·d)) in response to the higher activity of bacteria at higher temperature and NO_3-N dilution started after 10 days resulting from biomass and NOB washout, while NO_2-N stabilized at around 40–45 mg N/L. The NO_3-N and NO_2-N production were more than double in Fig. 3b in comparison to Fig. 3a based on higher activity of bacteria in higher temperature.

3.2. Feature selection for ML algorithms

Fig. 4 shows a heatmap of the PCC between the variables (N species, biomass components, and online measurements) and N_2O concentration (target variable). The highest positive and negative correlation, 0.82 and −0.56, was obtained for NH_4-N and NO_2-N, respectively. The biomass components (MLSS and MLVSS) with the correlation factor of 0.48 were the next highest correlated variables. However, both parameters (MLSS and MLVSS) had a perfect correlation of 1.0 between each other, and thus only one of them (MLSS) was considered in the final subset of features to avoid multicollinearity issues.

The results of the RF method were in line with the Pearson correlation concerning the highest importance level of the nitrogen species with the target variable (Fig. 5). The maximum importance levels were obtained for NH_4-N (0.71) and NO_2-N (0.37). Moreover, among the online measurements, DO concentration had the highest correlation with N_2O concentration for both examined methods.

3.3. ML modeling results

3.3.1. Model predictions against training data

All three examined prediction models were trained and tested based on the data from the experiment at 20 °C and 12 °C, respectively. The comparative results for all the training models are shown in Fig. 6a. The overall performance of the models was within an acceptable range (Table 2) The noisy data points were not predicted accurately as they were treated as outliers.

Each algorithm required a specific approach and trial-and-error attempt to obtain the optimum parameter set, which ensured a high prediction accuracy. The ANN model was developed after looping over 300 epochs on the training data set. The SVM model was built with the regularization parameter (C=1), and SVR epsilon tube (epsilon=0.1). For the GBM, the following setting was selected: 4000 estimators, the learning rate of 0.01, min. sample leaf of 40, min. sample split of 30, and max. depth of 40.

3.3.2. Model predictions against test data

The trained prediction models were tested by another data set (experiment at 12 °C) (Fig. 6b). The SVM and GBM were overfitted,

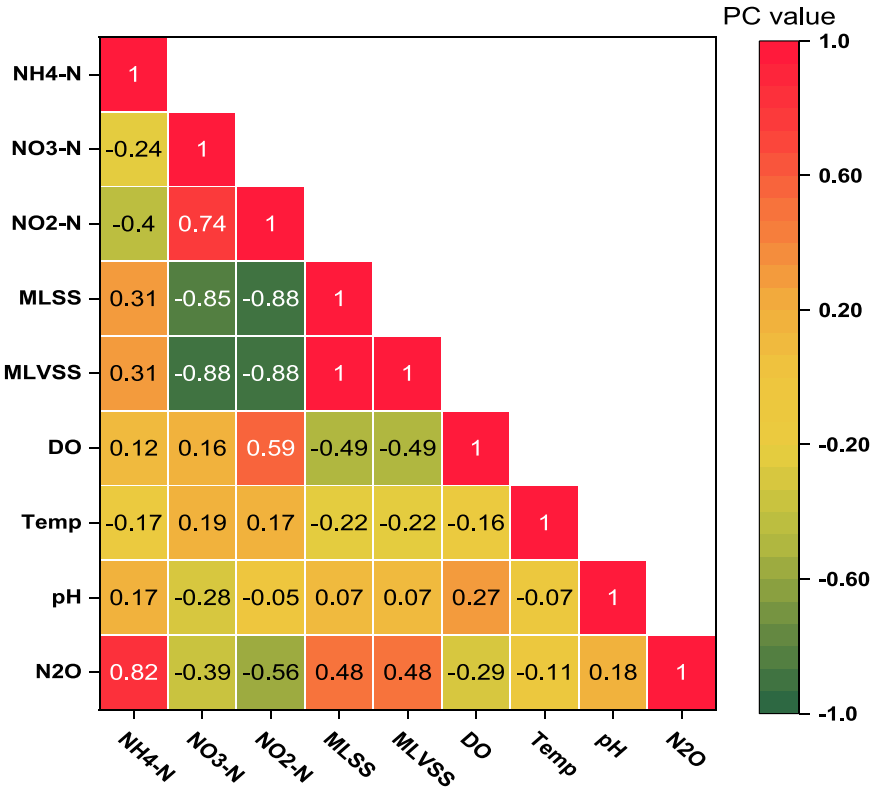

Fig. 4. Heatmap of Pearson correlation coefficient for input data with the target variable (N_2O).

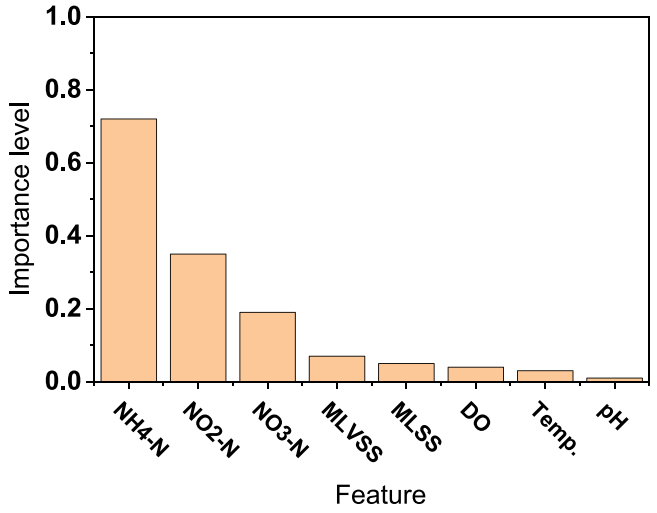

Fig. 5. RF feature selection importance level of the features related to N_2O production.

even though they were able to capture the train data patterns. On the other hand, the ANN demonstrated its versatility under the different operational conditions and process patterns. As shown in Fig. 6b, the SVM overestimated the N_2O peak with a 6-day delay, and the GBM failed to predict any distinguishable climax.

3.3.3. Model efficiency evaluation and comparison

Table 2 presents the efficiency and error of each prediction algorithm. The ANN had the highest coefficient of determination, i.e., $R^2_{Train=}0.93$, $R^2_{Test=}0.67$, and the lowest error indexes. These measures confirm that the ANN is the best model for predicting liquid N_2O concentrations during the experimental trials under different operational conditions. The SVM failed to predict the N_2O concentrations of unseen test data and the GBM partially detected the pattern

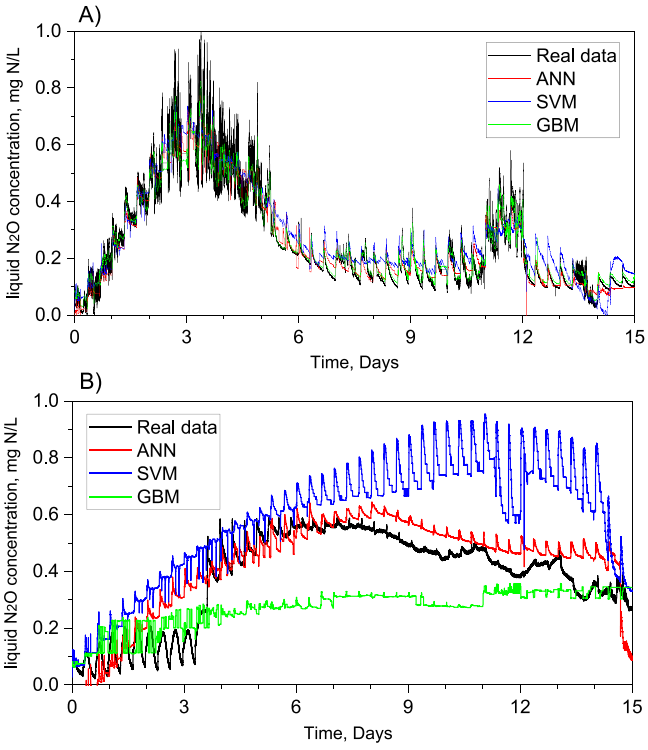

Fig. 6. Training and test results of the prediction models, (A) Train data (experiment at 20 °C), and (B) Test data (experiment at 12 °C).

of the real data at the beginning and end of the experiment. The high values of R^2_{Train} and low values of R^2_{Test} show that both SVM and GBM are overfitted and failed to predict the target variable. Among all the examined models, the ANN had also the best J^2, i.e., closest value to

Table 2
Model efficiency criteria for the examined prediction models.

Model	Training data				Test data				
	R^2	MSE	RMSE	MAE	R^2	MSE	RMSE	MAE	J^2
ANN	**0.92**	**0.002**	**0.048**	**0.006**	**0.67**	**0.012**	**0.09**	**0.002**	**1.87**
SVM	0.88	0.003	0.062	0.12	0.06	0.057	0.239	0.23	3.71
GBM	0.97	0.007	0.077	1.23	0.12	0.027	0.266	0.11	3.45

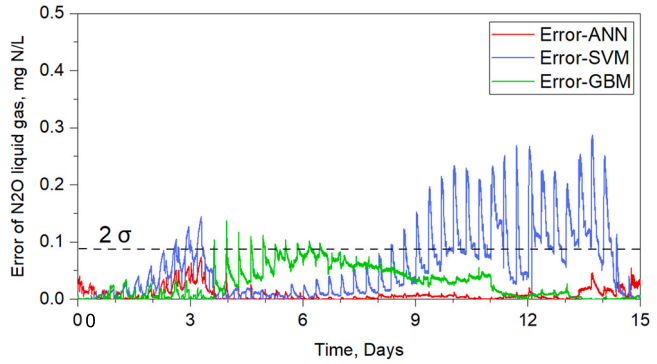

Fig. 7. Prediction errors of liquid N_2O concentrations for the examined prediction models from the test data (σ is the standard deviation of the test data set).

1.0. This confirms the ability of that model in finding data patterns under a highly dynamic behavior of the online measurements.

In Fig. 7, it can be seen that at the beginning of the experimental trial (days 2–4), the model outputs had considerable errors due to a sudden increase in N_2O production. After 4 days, when the stability in N_2O production was achieved, the errors (except for the SVM) became more stable. The ANN model output error was below the doubled standard deviation (2 σ) during the entire experiment, which indicated a valid and proper prediction (Fig. 7). Moreover, the variance of the prediction error in the ANN model was significantly lower than the SVM and GBM for the test data.

3.3.4. Confidence interval for the selected model (ANN)

The result of CI was evaluated based on the z-score as there was a large number of population and the Gaussian shape of the error distribution. Overall, the data values are mostly within the error range of ± 0.13 N_2O mg/L as an upper and lower band of 95% CI (Fig. 8). Moreover, the variance of ANN model prediction is located in the confidence region (95% CI), showing its accuracy. This confirms that the ANN model predicted the measured data with 95% of the observed uncertainty.

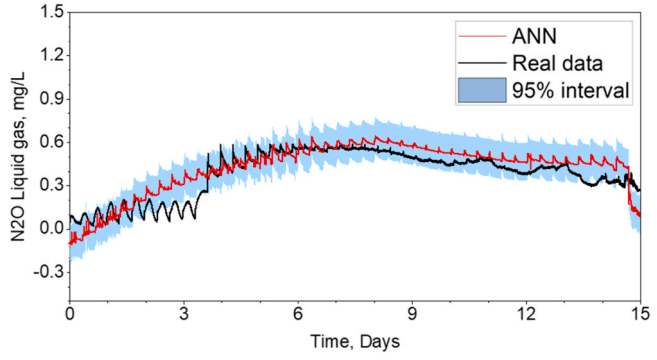

Fig. 8. Measured data, ANN model predictions and 95% confidence interval of the predictions.

3.3.5. Effect of mechanistic modeling (data acquisition) on the prediction performance

For evaluation of the effect of the mechanistic model on the ML prediction performance, the models were fed with the direct experimental data (without mechanistic modeling). It can be seen in the SI (Fig. S4) that only the SVM could train the model with the acceptable accuracy (R^2 =0.76), but failed to predict the test data set (R^2 =0.0). The ANN and GBM could not train the models nor predict the test data-set. Table S1 shows the efficiency and error for each prediction ML algorithm without considering the mechanistic model. Mechanistic modeling prior to the ML procedure had a significant impact on the accuracy of training and testing the N_2O prediction. In the ANN model, after applying mechanistic modeling before the ML prediction, the accuracy increased dramatically from R^2_{Test}= −0.06 (Table S1) to R^2_{Test}= 0.67 (Table 2). This improvement can be justified by the fact that ML models need a sufficiently large data-set first to train and then predict accurately the test data-set.

4. Discussion

Results of the feature selection analysis on N_2O production show that the behavior of NH_4-N and NO_2-N plays an important role in predicting N_2O accumulation during nitrification. This finding was supported by the results of other studies (Duan et al., 2020; Li et al., 2015; Song et al., 2020). Song et al. (2020) observed that NH_4-N and the sum of NO_2-N and NO_3-N had the highest effect on N_2O emissions in a feature selection study of a full-scale WWTP. Strong positive correlations between NH_4-N oxidation and N_2O production during nitrification were also reported in a pilot-scale SBR (Li et al., 2015) and full-scale SBR (Duan et al., 2020). Moreover, in the study of (Duan et al., 2020), a strong positive correlation was also found between liquid N_2O and NO_2-N concentration (Pearson correlation of 0.93).

Furthermore, Duan et al. (2020) observed that N_2O emission exhibited a clear pattern that followed the DO profile in an intermittent aeration mode (Pearson correlation of 0.74). In the present study, a weak negative correlation (−0.29) was also found between the DO concentration and N_2O production during continuous aeration at the low DO setpoint of 0.6 mg O_2/L. It should be emphasized, however, that the well-established favorable conditions for liquid N_2O production comprise low DO and high NO_2-N concentrations (Mannina et al., 2017; Massara et al., 2018; Peng et al., 2014; Vasilaki et al., 2020a).

In the present study, the observed correlation of N_2O production with pH and temperature was lower than other evaluated parameters. N_2O production presented a weak positive correlation of 0.18 with pH which was kept in the range of 7.0–7.5 (Fig. 4). Law et al. (2011) reported that N_2O production fluctuated with pH in the range of 6.0 and 8.5 while keeping the pH between 6.4 and 7.0 reduced N_2O production in a partial nitrification system with aerobic conditions (Law et al., 2011). It can be seen in Fig. 5 that the online measurement data (temperature, DO, and pH) had a lower importance level than nitrogen species and biomass concentrations for the prediction of N_2O production. Vasilaki et al. (2020a) found that under similar DO and pH concentrations, the average liquid N_2O conditions can vary substantially.

The trend of N_2O production was different in experiments for train and test of ML Algorithms. However, the ANN model successfully predict the N_2O production in a test experiment (Fig. 6a,b). This higher production of N_2O (up to 1.0 mg N/L) in the first week of train experiment (Fig. 6a) can due to higher NLR of 0.05 ± 0.01 g N/(L.d) in compare to the test experiment (0.02 ± 0.01 g N/(L.d)) (Fig. 6b).

Table 3 presents various N_2O prediction studies with different modeling approaches (mechanistic and ML) in lab-scale, pilot-scale, or full-scale WWTPs. The mechanistic models were mostly used for the prediction of lab-scale or pilot-scale systems, while the ML

Table 3
Summary of different studies on N_2O prediction in lab-scale or full-scale WWTP.

Prediction method	Model / Algorithm	Model Accuracy	System	Remarks	References
Mechanistic	A mathematical model based on AOB and HB processes	na	Lab- and pilot-scale	The model result showed that the contribution of heterotrophs to N_2O production decreased with the increasing DO concentrations.	(Wang et al., 2016)
	ASM2d-N_2O	na	Full-scale	N_2O hotspots (important rise and falls) were predicted theoretically by an extended ASM considering all the biological pathways for N_2O production.	(Massara et al., 2018)
	ASM2d	R^2 = 0.65	Lab-scale and pilot-scale	The model was used as a tool for assessing the multivariable problem of N_2O mitigation in a combined N-P activated sludge system.	(Zaborowska et al., 2019)
	Mathematical model (two-step nitrification, four step HD)	R^2 = 0.83–0.99	Batch experiment	In the best-fit model, which combined two-step nitrification and denitrification pathways, the contribution of heterotrophs to N_2O production was stronger than autotrophs.	(Domingo-Félez et al., 2017)
	ASM-ICE	R^2 = 0.94–0.98	Batch experiment	The model predicted that N_2O accumulation resulted from a faster drop of the N_2O reduction rate than the NO_2-N reduction rate.	(Ding et al., 2017)
	Extended ASM model	R^2_{Test}= 0.88	Full-scale	The integrated N_2O model, considering the nitrification/denitrification pathways, could predict N_2O production.	(Ni et al., 2015)
	Extended ASM model	R^2 = 0.10–0.53 RMSE= 0.4–1.14	Full-scale	Imbalanced distribution of flow rate between the two treatment lines did not result in a substantial increase in N_2O emissions for the particular WWTP and operational parameters, according to the N_2O simulation results.	(Solís et al., 2022)
	Extended ASM model	R^2 (NSE)= 0.3–0.33 RMSE= 0.38–0.41	Full-scale	The model estimated the N_2O in terms of liquid and gaseous N_2O emissions. This extended model indicated the essential function of heterotrophs. The N_2O emission factor (EF) for the examined plant was between 0.9% and 0.94% of the influent TN-load.	(Maktabifard et al., 2022)
Machine Learning	Back Propagation-ANN	R^2_{Test}= 0.81–94 MSE= 0.1–0.8	Full-scale / pilot-scale	The model was a convenient and feasible method for the prediction of N_2O emissions in a nitrifying-denitrifying system.	(Sun et al., 2017)
	DNN and LSTM	R^2_{DNN}= 0.86 R^2_{LSTM}= 0.94	Full-scale	In a comparative study, the LSTM-based forecasting model performed better than the DNN-based model in terms of model goodness-of-fit	(Hwangbo et al., 2021)
	SVM	na	Full-scale	The model predicted that N_2O emissions accounted for 7.6% of the total NH_4-N load (on average) in a sidestream SBR. N_2O was correlated with DO, influent NH_4-N load, and pH.	(Vasilaki et al., 2020a)
Hybrid method	Extended ASM1 and three different ML algorithms (ANN, SVM, and GBM)	ANN model: R^2_{Train}= 0.92 R^2_{Test}= 0.67 $RMSE_{Train}$= 0.048 $RMSE_{Test}$= 0.09	Lab-scale	NH_4-N and NO_2-N had the highest correlation with N_2O production. ANN revealed the best performance among other algorithms.	This study

na: not available, AOB: Ammonia oxidation bacteria, HB: heterotrophic bacteria, HD: heterotrophic denitrification, DNN: deep neural network, SVM: support vector machines, ANN: artificial neural network, CSTR: continuously stirred tank reactor, ASM-ICE: Activated Sludge Model for Indirect Coupling of Electrons, NSE: Nash-Sutcliff coefficient.

methods considered data from full-scale systems. In general, the accuracy of N_2O prediction was higher for the pure ML models than the pure mechanistic models, and the developed hybrid model of this study revealed one of the highest prediction accuracies in comparison with the studies shown in Table 3.

An accurate prediction of N_2O can play a significant role in the mitigation of N_2O from WWTPs (Solís et al., 2022; Maktabifard et al., 2022). Hence, the proposed approach, i.e., expanding a data set by a mechanistic model and prediction with ML algorithms, can be useful for the limited amounts of data collected during N_2O measurement campaigns towards a mitigation of this hazardous gas from the WWTPs. With sufficiently big data set, the ML algorithms can ensure predictions with a satisfactory level of performance (without expanding the data by a mechanistic model).

The present approach still has some limitations. Only the limited experimental data from a lab-scale system were considered, while the hybrid model still requires validation based on experimental data from full-scale WWTPs. Furthermore, nitrogen transformations were only evaluated with respect to nitrification, whereas denitrification may also be an important source of N_2O production in full-scale WWTPs. Expanding the input data of ML algorithms by external software, such as GPS-X, requires experiments to validate the mechanistic model. Furthermore, applicability of the hybrid models still requires further validation with more variety of data-sets.

For future studies, a comparison between mechanistic modeling and ML predictions for liquid N_2O production and gas N_2O emission in a bigger data set is suggested. Future ML algorithms can be developed for prediction of specific N_2O production pathways, although this function is now applicable only by mechanistic models. In addition, estimation of an N_2O emission factor, EF_{N2O}, can be another interesting and useful application for full-scale WWTPs. This factor plays a critical role in determining the WWTP carbon footprint (Maktabifard et al., 2020).

5. Conclusions

A hybrid model, combining mechanistic and ML (ANN) models, accurately predicted the liquid N_2O concentrations during two 15-day experimental trials in a nitrifying SBR. This approach is novel in comparison with the previous attempts for finding a predictive model of N_2O production during nitrification. The hybrid model successfully predicted unknown test data with an acceptable coefficient of determination (R^2_{TEST} = 0.67), showing its versatility in terms of variable operating conditions and the ability to generalize process patterns more accurately than the other two examined models (SVM, GBM). On the other hand, the SVM overfitted in the estimation of the test data and GBM failed to predict an acceptable model. Moreover, accounting for the level of uncertainty for the ANN model, the predicted values with more than 95% accuracy are reliable enough for delivering valuable information regarding the phenomenon for further research and practical applications. A hybrid modeling concept that combines mechanistic models of WWTPs (e.g., ASMs) with ML can be further expanded to predict N_2O production/emission in full-scale WWTPs for N_2O mitigation strategies.

Declaration of Competing Interest

The authors declare that they have no known competing financial interests or personal relationships that could have appeared to influence the work reported in this paper.

Acknowledgment

This work was supported by the Polish National Science Center, Poland under project no. UMO-2017/27/B/NZ9/01039.

Appendix A. Supporting information

Supplementary data associated with this article can be found in the online version at doi:10.1016/j.psep.2022.04.058.

References

Abbas, M.H., Norman, R., Charles, A., 2018. Neural network modelling of high pressure CO_2 corrosion in pipeline steels. Process Saf. Environ. Prot. 119, 36–45.
Al-Jamimi, H.A., Al-Azani, S., Saleh, T.A., 2018. Supervised machine learning techniques in the desulfurization of oil products for environmental protection: A review. Process Saf. Environ. Prot. 120, 57–71.
Alejo, L., Atkinson, J., Guzmán-Fierro, V., Roeckel, M., 2018. Effluent composition prediction of a two-stage anaerobic digestion process: machine learning and stoichiometry techniques. Environ. Sci. Pollut. Res. 25, 21149–21163.
Ali, M.M.M., Li, Z., Zhao, H., Rawashdeh, A., Al Hassan, M., Ado, M., 2021. Characterization of the health and environmental radiological effects of TENORM and radiation hazard indicators in petroleum waste –Yemen. Process Saf. Environ. Prot. 146, 451–463.
Alver, A., Altaş, L., 2017. Characterization and electrocoagulative treatment of landfill leachates: A statistical approach. Process Saf. Environ. Prot. 111, 102–111.
Arshad, U., Taqvi, S.A.A., Buang, A., Awad, A., 2021. SVM, ANN, and PSF modelling approaches for prediction of iron dust minimum ignition temperature (MIT) based on the synergistic effect of dispersion pressure and concentration. Process Saf. Environ. Prot. 152, 375–390.
Awad, M., Khanna, R., 2015. Support vector regression. In: Awad, M., Khanna, R. (Eds.), Efficient Learning Machines: Theories, Concepts, and Applications for Engineers and System Designers. Apress, Berkeley, CA, pp. 67–80.
Ayyadevara V.K., 2018, Gradient Boosting Machine. In: Pro Machine Learning Algorithms. Apress, Berkeley, CA.
Bagherzadeh, F., Mehrani, M.-J., Basirifard, M., Roostaei, J., 2021. Comparative study on total nitrogen prediction in wastewater treatment plant and effect of various feature selection methods on machine learning algorithms performance. Journal of Water Process Engineering 41.
Bagherzadeh, F., Shojaei Nouri, A., Mehrani, M.-J., Thennadil, S., 2021. Prediction of energy consumption and evaluation of affecting factorsin a full-scale WWTP using a machine learning approachFaramarz. Process Safety and Environmental Protection 154, 458–466. https://doi.org/10.1016/j.psep.2021.08.040
Breiman, L., 2001. Random forests. Mach. Learn. 45, 5–32.
Chen, K.H., Wang, H.C., Han, J.L., Liu, W.Z., Cheng, H.Y., Liang, B., Wang, A.J., 2020a. The application of footprints for assessing the sustainability of wastewater treatment plants: a review. J. Clean. Prod. 277, 124053.
Chen, H., Zeng, L., Wang, D., Zhou, Y., Yang, X., 2020b. Recent advances in nitrous oxide production and mitigation in wastewater treatment. Water Res 184, 116168.
Delre, A., ten Hoeve, M., Scheutz, C., 2019. Site-specific carbon footprints of Scandinavian wastewater treatment plants, using the life cycle assessment approach. J. Clean. Prod. 211, 1001–1014.
Ding, X., Zhao, J., Hu, B., Li, X., Ge, G., Gao, K., Chen, Y., 2017. Mathematical modeling of nitrous oxide (N2O) production in anaerobic/anoxic/oxic processes: Improvements to published N2O models. Chem. Eng. J. 325, 386–395.
Domingo-Félez, C., Pellicer-Nàcher, C., Petersen, M.S., Jensen, M.M., Plósz, B.G., Smets, B.F., 2017. Heterotrophs are key contributors to nitrous oxide production in activated sludge under low C-to-N ratios during nitrification—Batch experiments and modeling. Biotechnol. Bioeng. 114, 132–140.
Duan, H., van den Akker, B., Thwaites, B.J., Peng, L., Herman, C., Pan, Y., Ni, B.-J., Watt, S., Yuan, Z., Ye, L., 2020. Mitigating nitrous oxide emissions at a full-scale wastewater treatment plant. Water Res. 185, 116196.
Géron, A., 2019. Hands-On Machine Learning with Scikit-Learn, Keras, and TensorFlow, second ed., O'Reilly Media, Inc., 1005 Gravenstein Highway North, Sebastopol, CA, pp. 95472.
Haimi, H., Mulas, M., Corona, F., Vahala, R., 2013. Data-derived soft-sensors for biological wastewater treatment plants: An overview. Environ. Model. Softw. 47, 88–107.
Halim, S.Z., Quddus, N., Pasman, H., 2021. Time-trend analysis of offshore fire incidents using nonhomogeneous Poisson process through Bayesian inference. Process Saf. Environ. Prot. 147, 421–429.
Hauduc, H., Neumann, M.B., Muschalla, D., Gamerith, V., Gillot, S., Vanrolleghem, P.A., 2015. Efficiency criteria for environmental model quality assessment: A review and its application to wastewater treatment. Environ. Model. Softw. 68, 196–204.
Henze, M., Gujer, W., Mino, T., van Loosedrecht, M., 2006. Activated Sludge Models ASM1, ASM2, ASM2d and ASM3. IWA Publishing,.
Hogg, Rv, 2012. Introduction to Mathematical Statistics. Pearson.
Hvala, N., Kocijan, J., 2020. Design of a hybrid mechanistic/Gaussian process model to predict full-scale wastewater treatment plant effluent. Comput. Chem. Eng. 140, 106934.

Hwangbo, S., Al, R., Chen, X., Sin, G., 2021. Integrated Model for Understanding N2O Emissions from Wastewater Treatment Plants: A Deep Learning Approach. Environ. Sci. Technol. 55, 2143–2151.
Hydromantis, 2021. ⟨https://www.hydromantis.com/GPSX⟩. Canada.
IPCC, 2014, Intergovernmental Panel on Climate Change Fifth Assessment Report.
Kazemi, P., Bengoa, C., Steyer, J.-P., Giralt, J., 2021. Data-driven techniques for fault detection in anaerobic digestion process. Process Saf. Environ. Prot. 146, 905–915.
Koutsou, O.P., Gatidou, G., Stasinakis, A.S., 2018. Domestic wastewater management in Greece: greenhouse gas emissions estimation at country scale. J. Clean. Prod. 188, 851–859.
Law, Y., Lant, P., Yuan, Z., 2011. The effect of pH on N2O production under aerobic conditions in a partial nitritation system. Water Res. 45, 5934–5944.
Li, P., Wang, S., Peng, Y., Liu, Y., He, J., 2015. The synergistic effects of dissolved oxygen and pH on N2O production in biological domestic wastewater treatment under nitrifying conditions. Environ. Technol. 36, 1623–1631.
Maktabifard, M., Zaborowska, E., Makinia, J., 2020. Energy neutrality versus carbon footprint minimization in municipal wastewater treatment plants. Bioresour. Technol. 300, 122647.
Maktabifard, M., Blomberg, K., Zaborowska, E., Mikola, A., Mąkinia, J., 2022. Model-based identification of the dominant N2O emission pathway in a full-scale activated sludge system. J. Clean. Prod. 336, 130347.
Mannina, G., Capodici, M., Cosenza, A., Di Trapani, D., van Loosdrecht, M.C.M., 2017. Nitrous oxide emission in a University of Cape Town membrane bioreactor: The effect of carbon to nitrogen ratio. J. Clean. Prod. 149, 180–190.
Mannina, G., Rebouças, T.F., Cosenza, A., Chandran, K., 2019. A plant-wide wastewater treatment plant model for carbon and energy footprint: model application and scenario analysis. J. Clean. Prod. 217, 244–256.
Masmoudi, S., Elghazel, H., Taieb, D., Yazar, O., Kallel, A., 2020. A machine-learning framework for predicting multiple air pollutants' concentrations via multi-target regression and feature selection. Sci. Total Environ. 715, 136991.
Massara, T.M., Solís, B., Guisasola, A., Katsou, E., Baeza, J.A., 2018. Development of an ASM2d-N2O model to describe nitrous oxide emissions in municipal WWTPs under dynamic conditions. Chem. Eng. J. 335, 185–196.
Mehrani, M.-J., Lu, X., Kowal, P., Sobotka, D., Mąkinia, J., 2021. Incorporation of the complete ammonia oxidation (comammox) process for modeling nitrification in suspended growth wastewater treatment systems. J. Environ. Manag. 297, 113223.
Natekin, A., Knoll, A., 2013. Gradient boosting machines, a tutorial. Front. Neurorobotics 7.
Ni, B.-J., Pan, Y., van den Akker, B., Ye, L., Yuan, Z., 2015. Full-scale modeling explaining large spatial variations of nitrous oxide fluxes in a step-feed plug-flow wastewater treatment reactor. Environ. Sci. Technol. 49, 9176–9184.
Osarogiagbon, A.U., Khan, F., Venkatesan, R., Gillard, P., 2021. Review and analysis of supervised machine learning algorithms for hazardous events in drilling operations. Process Saf. Environ. Prot. 147, 367–384.
Park, J., Forman, B.A., Lievens, H., 2021. Prediction of active microwave backscatter over snow-covered terrain across western colorado using a land surface model and support vector machine regression. IEEE J. Sel. Top. Appl. Earth Obs. Remote Sens. 14, 2403–2417.
Peng, L., Ni, B.-J., Erler, D., Ye, L., Yuan, Z., 2014. The effect of dissolved oxygen on N2O production by ammonia-oxidizing bacteria in an enriched nitrifying sludge. Water Res. 66, 12–21.
Ranjan, K.G., Prusty, B.R., Jena, D., 2021. Review of preprocessing methods for univariate volatile time-series in power system applications. Electr. Power Syst. Res. 191, 106885.
Ryan, M., Müller, C., Di, H.J., Cameron, K.C., 2004. The use of artificial neural networks (ANNs) to simulate N2O emissions from a temperate grassland ecosystem. Ecol. Model. 175, 189–194.
Shaahmadi, F., Anbaz, M.A., Bazooyar, B., 2017. Analysis of intelligent models in prediction nitrous oxide (N2O) solubility in ionic liquids (ILs). J. Mol. Liq. 246, 48–57.
Smola, A.J., Schölkopf, B., 2004. A tutorial on support vector regression. Stat. Comput. 14, 199–222.
Song, M.J., Choi, S., Bae, W.B., Lee, J., Han, H., Kim, D.D., Kwon, M., Myung, J., Kim, Y.M., Yoon, S., 2020. Identification of primary effecters of N2O emissions from full-scale biological nitrogen removal systems using random forest approach. Water Res. 184, 116144.
Solís, B., Guisasola, A., Pijuan, M., Corominas, L., Baeza, J.A., 2022. Systematic calibration of N2O emissions from a full-scale WWTP including a tracer test and a global sensitivity approach. Chem. Eng. J. 435, 134733.
Steinwart, I., Christmann, A., 2008. Support Vector Machines. Springer, New York.
Su, Q., Domingo-Félez, C., Jensen, M.M., Smets, B.F., 2019. Abiotic Nitrous Oxide (N2O) Production Is Strongly pH Dependent, but Contributes Little to Overall N2O Emissions in Biological Nitrogen Removal Systems. Environ. Sci. Technol. 53, 3508–3516.
Sun, S., Bao, Z., Li, R., Sun, D., Geng, H., Huang, X., Lin, J., Zhang, P., Ma, R., Fang, L., Zhang, X., Zhao, X., 2017. Reduction and prediction of N2O emission from an Anoxic/Oxic wastewater treatment plant upon DO control and model simulation. Bioresour. Technol. 244, 800–809.
Vasilaki, V., Conca, V., Frison, N., Eusebi, A.L., Fatone, F., Katsou, E., 2020a. A knowledge discovery framework to predict the N2O emissions in the wastewater sector. Water Res. 178, 115799.
Vasilaki, V., Danishvar, S., Mousavi, A., Katsou, E., 2020b. Data-driven versus conventional N2O EF quantification methods in wastewater; how can we quantify reliable annual EFs? Comput. Chem. Eng. 141, 106997.
Vasilaki, V., Massara, T.M., Stanchev, P., Fatone, F., Katsou, E., 2019. A decade of nitrous oxide (N2O) monitoring in full-scale wastewater treatment processes: A critical review. Water Res. 161, 392–412.
Vapnik, V., Guyon, I., Hastie, T., 1995. Support vector machines. Mach. Learn 20, 273–297.
Verma, A., Wei, X., Kusiak, A., 2013. Predicting the total suspended solids in wastewater: A data-mining approach. Eng. Appl. Artif. Intell. 26, 1366–1372.
Wang, Q., Ni, B.-J., Lemaire, R., Hao, X., Yuan, Z., 2016. Modeling of Nitrous Oxide Production from Nitritation Reactors Treating Real Anaerobic Digestion Liquor. Sci. Rep. 6, 25336.
Wisniewski, K., Kowalski, M., Makinia, J., 2018. Modeling nitrous oxide production by a denitrifying-enhanced biologically phosphorus removing (EBPR) activated sludge in the presence of different carbon sources and electron acceptors. Water Res. 142, 55–64.
Xenochristou, M., Hutton, C., Hofman, J., Kapelan, Z., 2020. Water Demand Forecasting Accuracy and Influencing Factors at Different Spatial Scales Using a Gradient Boosting Machine. Water Resour. Res. 56 e2019WR026304.
Yegnanarayana, B., 2009. Artificial Neural Networks. PHI Learning Pvt. Ltd.
Zaborowska, E., Lu, X., Makinia, J., 2019. Strategies for mitigating nitrous oxide production and decreasing the carbon footprint of a full-scale combined nitrogen and phosphorus removal activated sludge system. Water Res. 162, 53–63.